Journal of Sound and Vibration (2002) **255**(3), 433–456
doi:10.1006/jsvi.2001.4164, available online at http://www.idealibrary.com on IDEAL®

A GEOMETRICALLY NON-LINEAR MODEL OF ROTATING SHAFTS WITH INTERNAL RESONANCE AND SELF-EXCITED VIBRATION

J. ŁUCZKO

Institute of Mechanics and Machine Design, Cracow University of Technology, Al. Jana Pawła II-go 37, *PL*-31-864 *Kraków Poland. E-mail: jluczko@mech.pk.edu.pl*

(*Received* 4 *January* 2001, *and in final form* 3 *August* 2001)

A geometrically non-linear model of the rotating shaft is introduced, which includes Kárman non-linearity, non-linear curvature effects, large displacements and rotations as well as gyroscopic effects. Through applying Timoshenko-type assumptions, the shear effects are also included in the model. Convenient matrix descriptions are used in order to facilitate the analysis based on Galerkin and continuation methods. The model is used to analyze the phenomenon of internal resonance. The influence of some of the system's parameters on the amplitude and frequency of self-excited vibration is investigated.

1. INTRODUCTION

In order to analyze the physical phenomena in shafts rotating with a velocity close to the critical rotation speed it is necessary to use non-linear models, which due to the large amplitudes of vibration should consider the effect of geometrical non-linearities. For shafts made of a material with very small internal damping, very interesting steady state vibration phenomena can be excited. They can be explained on the basis of the phenomenon of internal resonance.

Also very important is the influence of internal damping, which has a destabilizing effect and can cause self-excited vibrations [1, 2]. Another factor, which can have a destabilizing effect on the system is a constant external loading, especially of the follower type. This class of load can comprise the axial force described, e.g., in reference [3] and the torque applied to the shaft, which is the main load transmitting power in the angular motion. The torque has an important effect on the stability regions and in a general case its presence reduces the system's critical speed [4].

In the analysis of non-linear phenomena the Euler-type models of slender shafts are considered. In this case, the non-linearity is the result of the influence of the axial force on the transversal vibrations. Shaw and Shaw [5] considered the problem of bifurcations in a rotating shaft, using a non-linear model. The shaft has been modelled as an Euler beam with Kárman non-linearity, simply supported at both ends. A similar model, but with a rigid disk attached at the shaft middle point was also considered by Chang and Cheng [6]. In both these works, the center manifold theory has been used to obtain analytical formulae combining the system's parameters, the frequency and the amplitude of vibration.

In the papers by Chen and Sheu [3], Han and Zu [7] as well as by Lee *et al.* [8], the shaft has been modelled as a Timoshenko beam, but with consideration of internal damping or geometrical non-linearities. Unfortunately, the analysis of a linear system is not suitable for

0022-460X/02/$35.00

predicting the amplitudes of self-excited vibration. To this end, it is necessary to consider a non-linear model accounting for geometrical constrains, which limits the amplitude of vibration. By additionally modelling the effect of the torque and the axial force, one has to consider a spatial model, which describes the coupled flexural, axial and torsional vibrations.

In the present paper a geometrically non-linear model of a rotating shaft is considered, which accounts for both large displacements and rotations as well as for large deformations. The formulation is based on the Timoshenko–Reissner model [9] and the modelling approach of Simo and Vu-Quoc [10] is used. In spite of the assumed simplification, the present model describes more exactly the influence of the geometrical constraints than models investigated upto now. Additionally, the influence of shear, rotational and longitudinal inertia and external and internal damping is considered. The model allows investigation of coupled torsional, longitudinal and flexural vibrations.

The method of analysis applied in the present paper is based on the Galerkin method. As a result of discretization of the system the analysis is reduced to the investigation of the so-called "matrix amplitude equation" [11, 12] which describes the non-linear eigenvalue problem. Thanks to application of some properties of the Kronecker product [13] the form of matrix amplitude equation obtained can be described by matrices independent of state vector co-ordinates. It allows simple prediction of the tangent matrix used in the iterative solution of the non-linear eigenvalue problem. To solve this problem continuation methods are usually applied [14–22].

A theoretical basis of the continuation methods and bifurcation analysis can be found in the book by Seydel [14]. The important works in the domain on the non-linear eigenvalue problems and the numerical bifurcation analysis of periodic solutions were published by Shroff and Keller [15], Doedel *et al.* [16, 17] and Meerbergen and Roose [18].

The approach to the analysis of the phenomena of internal resonance used in the present paper is similar to that described e.g., in the papers by Lewandowski [11, 12] and Leung and Fung [19], which concern the problem of the bifurcation of the solutions which describe the free vibrations of slender beams.

Another approach to the bifurcation analysis was applied in papers [15–18, 20–22]. In these papers, the authors deal with the efficient computation and bifurcation analysis of periodic solutions of large-scale dynamical systems and the determination of their stability. These systems are results of space discretization of partial differential equations. To solve the non-linear two-boundary problem the multiple-shooting or single-shooting methods [20], collocations and finite difference techniques [22] are applied. In spite of longer numerical calculation time, the methods described in papers [15–18, 20–22] are more general. These methods make possible bifurcation analysis of solutions for considerably wider classes of dynamical systems.

After a short description of the model, a method is discussed whereby the problem of solving the partial differential equations which describe the dynamics of the system is reduced to an algebraic non-linear problem. Based on the continuation methods some dynamical characteristics describing the phenomenon of internal resonance and self-excited vibrations were obtained.

2. THE MODEL OF THE SYSTEM

2.1. MAIN ASSUMPTIONS. GENERAL FORM OF THE EQUATIONS OF MOTION

In the derivation of the equations of motion it is helpful, especially for spatial beam models, to introduce a moving co-ordinate system rigidly connected to the shaft cross-section [23], the so-called body frame shown in Figure 1.

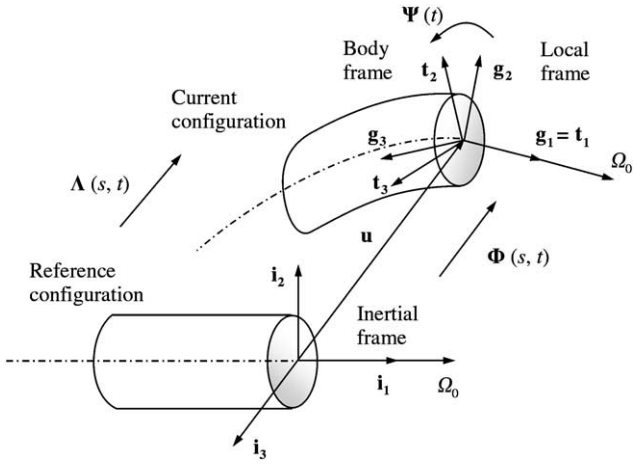

Figure 1. Reference and current configuration.

By introducing the body frame, the description of the motion of a continuous system can be reduced to the analysis of the motion of a co-ordinate system, the position of which is given at any time by the displacement vector $\mathbf{u}$ and the rotation matrix $\mathbf{\Lambda}$. In order to define the strain tensor and the internal forces and moments, one considers two configurations: the current configuration for the deformed state and the reference configuration for the undeformed state. In most analyses of the vibration of beams one also assumes that the deformation of the beam cross-section can be neglected. It is possible to derive the equations of motion by applying the balance of momentum and angular momentum in the current configuration, as discussed in references [23, 24]. By applying this approach, one obtains in a general case the following system of matrix equations:

$$\mathbf{B}_1\ddot{\mathbf{u}} + \mu_e\dot{\mathbf{u}} = \mathbf{\Lambda}(\mathbf{n}' + \tilde{\boldsymbol{\varepsilon}}_r\mathbf{n}), \qquad \mathbf{B}_2\dot{\boldsymbol{\omega}} + \tilde{\boldsymbol{\omega}}B_2\boldsymbol{\omega} = \mathbf{m}' + \tilde{\boldsymbol{\varepsilon}}_r\mathbf{m} + (\tilde{\mathbf{e}}_1 + \tilde{\boldsymbol{\varepsilon}}_t)\mathbf{n}. \tag{1}$$

In equations (1), the time derivatives with respect to time are denoted by a dot, whereas a prime stands for the spatial derivatives with respect to the natural co-ordinate s. Moreover, a matrix notation of the cross product has been used $\mathbf{a}\times\mathbf{b} = \tilde{\mathbf{a}}\mathbf{b}$, where in a general case the skew-symmetric matrix $\tilde{\mathbf{a}}$ is related to a vector $\mathbf{a}$ as

$$\tilde{\mathbf{a}} = \begin{bmatrix} 0 & -a_3 & a_2 \\ a_3 & 0 & -a_1 \\ -a_2 & a_1 & 0 \end{bmatrix}, \qquad \mathbf{a} = \begin{Bmatrix} a_1 \\ a_2 \\ a_3 \end{Bmatrix}. \tag{2}$$

To introduce the notation used in the sequel, a skew-symmetric matrix $\tilde{\mathbf{e}}_1$ corresponds by relation (2) to a unit vector tangent to the beam axis in the reference configuration. The matrix $\tilde{\boldsymbol{\omega}} = \mathbf{\Lambda}^{\mathrm{T}}\dot{\mathbf{\Lambda}}$ defines by formula (2) the angular velocity vector $\boldsymbol{\omega}$ in the body frame. In the sequel, one also uses two inertia matrices $\mathbf{B}_1 = \rho A\mathbf{I}$ and $\mathbf{B}_2$. The second of these matrices represents the tensor of the moments of inertia of the cross-section and is diagonal in the case when the co-ordinate axes coincide the principal axes. Moreover, the symbol μ_e will stand for the coefficient of external damping.

Important non-linear terms appearing in equation (1) are the terms $\tilde{\boldsymbol{\omega}}\mathbf{B}_2\boldsymbol{\omega}$, responsible for the gyroscopic effects. The equations in form (1) are also valid in the case of large rotations of the shaft cross-sections. In this case, there is an effect of the terms which include the

rotation matrix $\mathbf{\Lambda}$. The rotation matrix is a non-linear function of the rotation pseudovector, as will be discussed later on. Additional non-linear terms will result after considering the physical relations between the generalized forces $\mathbf{n}$, $\mathbf{m}$ and the deformation vectors $\boldsymbol{\varepsilon}_t$, $\boldsymbol{\varepsilon}_r$, which are also non-linear functions of the displacement and rotation vectors. The vector $\boldsymbol{\varepsilon}_t$ mostly includes the effects of axial deformation and shear in accordance with the Timoshenko model (translation of the body frame), whereas the vector $\boldsymbol{\varepsilon}_r$ describes the beam bending and torsion (rotation). The vectors $\boldsymbol{\varepsilon}_t$, $\boldsymbol{\varepsilon}_r$ are defined as in reference [23], by the relations

$$\boldsymbol{\varepsilon}_t = \mathbf{\Lambda}^{\mathrm{T}}(\mathbf{u}' + \mathbf{e}_1) - \mathbf{e}_1, \qquad \tilde{\boldsymbol{\varepsilon}}_r = \mathbf{\Lambda}^{\mathrm{T}}\mathbf{\Lambda}'. \tag{3}$$

The vector $\boldsymbol{\varepsilon}_r$ is related to the skew-symmetric matrix $\tilde{\boldsymbol{\varepsilon}}_r$ by the general rule (2). The relations given by equations (3) have been derived by assuming that the beam cross-sections do not undergo warping.

By introducing an auxiliary vector $\boldsymbol{\varepsilon} = [\varepsilon_{11}, 2\varepsilon_{12}, 2\varepsilon_{13}]^{\mathrm{T}}$, the components of which include the non-zero components of the strain tensor, one can write the $\boldsymbol{\varepsilon}$ vector in the form

$$\boldsymbol{\varepsilon} = (\mathbf{I} + \tfrac{1}{2}\mathbf{e}_1\boldsymbol{\varepsilon}_0^{\mathrm{T}})\boldsymbol{\varepsilon}_0, \tag{4}$$

where

$$\boldsymbol{\varepsilon}_0 = \boldsymbol{\varepsilon}_t + \tilde{\boldsymbol{\varepsilon}}_r\boldsymbol{\eta} = \boldsymbol{\varepsilon}_t + \tilde{\boldsymbol{\eta}}^{\mathrm{T}}\boldsymbol{\varepsilon}_r. \tag{5}$$

Here $\boldsymbol{\eta}$ is a vector which describes the position of a point in the system rigidly connected with the beam cross-section (the body frame). After introducing relations (3) and (5) into equation (4) one can show that the components of the $\boldsymbol{\varepsilon}$ vector are identical as those used, e.g., in reference [25].

The use of the auxiliary vector $\boldsymbol{\varepsilon}$ helps to facilitate considerably the further description of the model. Using this vector, and assuming linear physical relations between the stresses and deformations, one can write the constitutive equations in the form

$$\boldsymbol{\sigma} = \mathbf{E}(\boldsymbol{\varepsilon} + \mu_i\dot{\boldsymbol{\varepsilon}}). \tag{6}$$

Here $\boldsymbol{\sigma} = [\sigma_{11}, \sigma_{12}, \sigma_{13}]^{\mathrm{T}}$, and μ_i is the coefficient of internal damping. The components of the diagonal matrix $\mathbf{E} = \mathrm{diag}(E, kG, kG)$ depend on Young's modulus E, the shear modulus G and the shear factor k. By using equations (4) and (6) it is possible to calculate the vector of the generalized forces defined in the body frame as

$$\mathbf{n} = \int_A \boldsymbol{\sigma}\,\mathrm{d}A, \qquad \mathbf{m} = \int_A \tilde{\boldsymbol{\eta}}\boldsymbol{\sigma}\,\mathrm{d}A. \tag{7}$$

Here $\boldsymbol{\eta} = x_2\mathbf{e}_2 + x_3\mathbf{e}_3$ and $\mathrm{d}A = \mathrm{d}x_2\,\mathrm{d}x_3$. It can be seen that the variables of integration appear in the matrix $\tilde{\boldsymbol{\eta}}$. Moreover, this matrix is also a part of definition (5) of the vector $\boldsymbol{\varepsilon}_0$, which then defines $\boldsymbol{\sigma}$ by relations (4), (6). After the necessary integrations, and assuming that the integrals including odd powers of $\tilde{\boldsymbol{\eta}}$ (e.g., the static moments of the cross-section) vanish, one obtains

$$\begin{aligned}\mathbf{n} &= \mathbf{J}_1(\boldsymbol{\varepsilon}_t + \mu_i\dot{\boldsymbol{\varepsilon}}_t) + \mathbf{J}_1\mathbf{e}_1\boldsymbol{\varepsilon}_t^{\mathrm{T}}(\tfrac{1}{2}\boldsymbol{\varepsilon}_t + \mu_i\dot{\boldsymbol{\varepsilon}}_t) + \mathbf{J}_1\mathbf{e}_1\boldsymbol{\varepsilon}_r^{\mathrm{T}}\mathbf{J}_0(\tfrac{1}{2}\boldsymbol{\varepsilon}_r + \mu_i\dot{\boldsymbol{\varepsilon}}_r),\\ \mathbf{m} &= \mathbf{J}_2(\boldsymbol{\varepsilon}_r + \mu_i\dot{\boldsymbol{\varepsilon}}_r) + \mathbf{J}_2\tilde{\mathbf{e}}_1(\tilde{\boldsymbol{\varepsilon}}_r\boldsymbol{\varepsilon}_t - \mu_i\tilde{\boldsymbol{\varepsilon}}_t\dot{\boldsymbol{\varepsilon}}_r + \mu_i\tilde{\boldsymbol{\varepsilon}}_r\dot{\boldsymbol{\varepsilon}}_t).\end{aligned} \tag{8}$$

The $\mathbf{J}_k$ matrices ($k = 1, \ldots, 3$) are diagonal matrices in the case of beams with a circular cross-section. The components of the $\mathbf{J}_1 = \mathbf{E}A$ matrix include the axial stiffness and two

shear stiffnesses, those of the $\mathbf{J}_2$ matrix include the torsional stiffness and the bending stiffnesses. The matrices $\mathbf{J}_0$ and $\mathbf{J}_2$ can be defined as

$$\mathbf{J}_0 = \frac{1}{A}\int_A \tilde{\boldsymbol{\eta}}\tilde{\boldsymbol{\eta}}^{\mathrm{T}}\,\mathrm{d}A, \qquad \mathbf{J}_2 = \int_A \tilde{\boldsymbol{\eta}}\mathbf{E}\tilde{\boldsymbol{\eta}}^{\mathrm{T}}\,\mathrm{d}A. \tag{9}$$

The non-linear term of the $\mathbf{n}$ vector including the $\boldsymbol{\varepsilon}_t$ vector is of much importance in the analysis of vibration, especially when shear effects are taken into account and for the boundary conditions when the two beam ends cannot displace. The discussed non-linear term accounts for the non-linear dependence of the axial force on the derivatives of the transverse displacement and is the frequently analyzed Kárman non-linearity. The remaining non-linear terms, which depend on the $\boldsymbol{\varepsilon}_r$ vector, can become important in the analysis of spatial beams in the presence of coupling between the flexural, torsional and longitudinal modes. The system of equations (1), (8) with definitions (3) describes a non-linear, geometrically exact model of the analyzed system.

2.2. THE EQUATIONS OF MOTION OF THE SHAFT

The undisturbed angular motion of the shaft, in the absence of vibration, can be described by the rotation matrix given in the simple form

$$\boldsymbol{\Psi}(t) = \begin{bmatrix} 1 & 0 & 0 \\ 0 & \cos\psi(t) & -\sin\psi(t) \\ 0 & \sin\psi(t) & \cos\psi(t) \end{bmatrix}, \tag{10}$$

in the case of rotation with a constant speed $\psi(t) = \Omega_0 t$. In the presence of vibration, after the excitation of free, forced or self-excited vibration, the absolute motion of the shaft can be considered as a superposition of a rotation about a steady axis and of the motion resulting from vibration. This absolute motion will be further characterized by the rotation matrix, assumed to be of the form

$$\boldsymbol{\Lambda}(s,t) = \boldsymbol{\Phi}(s,t)\,\boldsymbol{\Psi}(t). \tag{11}$$

The rotation matrix $\boldsymbol{\Phi}$ describes the rotation of the local frame with respect to the inertial frame, whereas the matrix $\boldsymbol{\Psi}$ describes the motion of the body frame with respect to the local frame (Figure 1). The equations of motion of the shaft are obtained by introducing form (11) of the $\boldsymbol{\Lambda}$ matrix into equation (1) and (3). Moreover, it is necessary to express the vector $\boldsymbol{\omega}$, which is related to the matrix $\tilde{\boldsymbol{\omega}} = \boldsymbol{\Lambda}^{\mathrm{T}}\dot{\boldsymbol{\Lambda}}$, by the vectors $\boldsymbol{\Omega}$ (which describes vibration) and $\boldsymbol{\Omega}_0$ (which describes the shaft rotation). For the vector $\boldsymbol{\omega}$ one gets

$$\boldsymbol{\omega} = \boldsymbol{\Psi}^{\mathrm{T}}\boldsymbol{\Omega} + \boldsymbol{\Omega}_0 = \boldsymbol{\Psi}^{\mathrm{T}}(\boldsymbol{\Omega} + \boldsymbol{\Omega}_0). \tag{12}$$

Here one uses the fact that for the rotation matrix in the form (10), the vector $\boldsymbol{\Omega}_0 = \boldsymbol{\Psi}^{\mathrm{T}}\boldsymbol{\Omega}_0 = \Omega_0\mathbf{e}_1$. The time derivative of the vector $\boldsymbol{\omega}$ is given by the formula

$$\dot{\boldsymbol{\omega}} = \boldsymbol{\Psi}^{\mathrm{T}}(\dot{\boldsymbol{\Omega}} + \tilde{\boldsymbol{\Omega}}_0^{\mathrm{T}}\boldsymbol{\Omega}). \tag{13}$$

Since expressions (11–13) include the time-dependent rotation matrix $\boldsymbol{\Psi}(t)$, the resulting equations will, in general, be non-linear parametric equations. Under some assumptions, mainly about the shape of the beam cross-section (axial symmetry), one can obtain

equations with the coefficients which are independent of time. To this end, the vectors $\boldsymbol{\varepsilon}_t$ and $\boldsymbol{\varepsilon}_r$ can be written in the form

$$\boldsymbol{\varepsilon}_t = \boldsymbol{\Psi}^{\mathrm{T}}\boldsymbol{\tau}_t, \qquad \boldsymbol{\varepsilon}_r = \boldsymbol{\Psi}^{\mathrm{T}}\boldsymbol{\tau}_r, \tag{14}$$

where

$$\boldsymbol{\tau}_t = \boldsymbol{\Phi}^{\mathrm{T}}\mathbf{u}' + (\boldsymbol{\Phi}^{\mathrm{T}} - \mathbf{I})\mathbf{e}_1, \qquad \tilde{\boldsymbol{\tau}}_r = \boldsymbol{\Phi}^{\mathrm{T}}\boldsymbol{\Phi}'. \tag{15}$$

In order to calculate the generalized internal forces (8) it is necessary to calculate the time velocities of vectors (14), which are found to be equal to

$$\dot{\boldsymbol{\varepsilon}}_t = \boldsymbol{\Psi}^{\mathrm{T}}(\dot{\boldsymbol{\tau}}_t + \tilde{\boldsymbol{\Omega}}_0^{\mathrm{T}}\boldsymbol{\tau}_t), \qquad \dot{\boldsymbol{\varepsilon}}_r = \boldsymbol{\Psi}^{\mathrm{T}}(\dot{\boldsymbol{\tau}}_r + \tilde{\boldsymbol{\Omega}}_0^{\mathrm{T}}\boldsymbol{\tau}_r). \tag{16}$$

Equations (16) are the matrix form of the vector expressions between the local and global derivatives. Similar to equations (14), one can write the internal forces in the form

$$\mathbf{n} = \boldsymbol{\Psi}^{\mathrm{T}}(\mathbf{N} + \mathbf{N}_0), \qquad \mathbf{m} = \boldsymbol{\Psi}^{\mathrm{T}}(\mathbf{M} + \mathbf{M}_0). \tag{17}$$

Equations (17) include the constant terms $\mathbf{N}_0$ and $\mathbf{M}_0$. By making use of equations (11–17) one can then transform equations (1) and (8) to a form in which the matrix $\boldsymbol{\Psi}(t)$ appears only in the expressions

$$\mathbf{J}_k^t = \boldsymbol{\Psi}\mathbf{J}_k\boldsymbol{\Psi}^{\mathrm{T}}, \qquad \mathbf{B}_k^t = \boldsymbol{\Psi}\mathbf{B}_k\boldsymbol{\Psi}^{\mathrm{T}}. \tag{18}$$

In the case of a shaft of circular cross-section, matrices (18) are independent of time ($\mathbf{J}_k^t = \mathbf{J}_k$, $\mathbf{B}_k^t = \mathbf{B}_k$). Therefore, the parametric effects can show in the absence of symmetry of the elastic properties (the matrices $\mathbf{J}_k^t$) or of the inertial properties (the matrices $\mathbf{B}_k^t$). The final form of the equations of motion used in the subsequent analysis has the form

$$\begin{aligned} &\mathbf{B}_1^t\ddot{\mathbf{u}} + \mu_e\dot{\mathbf{u}} = \boldsymbol{\Phi}(\mathbf{N}' + \tilde{\boldsymbol{\tau}}_r\mathbf{N} - \tilde{\mathbf{N}}_0\boldsymbol{\tau}_r),\\ &\mathbf{B}_2^t\dot{\boldsymbol{\Omega}} + \mathbf{B}_g\boldsymbol{\Omega} + \tilde{\boldsymbol{\Omega}}\mathbf{B}_2^t\boldsymbol{\Omega} = \mathbf{M}' + \tilde{\boldsymbol{\tau}}_r\mathbf{M} + (\tilde{\mathbf{e}}_1 + \tilde{\boldsymbol{\tau}}_t)\mathbf{N} - \tilde{\mathbf{M}}_0\boldsymbol{\tau}_r - \tilde{\mathbf{N}}_0\boldsymbol{\tau}_t. \end{aligned} \tag{19}$$

Here,

$$\mathbf{B}_g(\boldsymbol{\Omega}_0) = \mathbf{B}_2^t\tilde{\boldsymbol{\Omega}}_0^{\mathrm{T}} + \tilde{\boldsymbol{\Omega}}_0\mathbf{B}_2^t - \widetilde{(\mathbf{B}_2^t\boldsymbol{\Omega}_0)}. \tag{20}$$

The matrix $\mathbf{B}_g$ describes the gyroscopic effects. The equations for the generalized forces $\mathbf{N}$, $\mathbf{M}$ have a similar structure as equations (8) discussed earlier

$$\begin{aligned} \mathbf{N} &= \mathbf{J}_1^t(\mathbf{U}\boldsymbol{\tau}_t + \mu_i\dot{\boldsymbol{\tau}}_t) + \mathbf{J}_1^t\mathbf{e}_1\boldsymbol{\tau}_t^{\mathrm{T}}(\tfrac{1}{2}\boldsymbol{\tau}_t + \mu_i\dot{\boldsymbol{\tau}}_t) + \mathbf{J}_1^t\mathbf{e}_1\boldsymbol{\tau}_r^{\mathrm{T}}\mathbf{J}_0^t(\tfrac{1}{2}\boldsymbol{\tau}_r + \mu_i\dot{\boldsymbol{\tau}}_r),\\ \mathbf{M} &= \mathbf{J}_2^t(\mathbf{U}\boldsymbol{\tau}_r + \mu_i\dot{\boldsymbol{\tau}}_r) + \mathbf{J}_2^t\tilde{\mathbf{e}}_1(\mathbf{U}\tilde{\boldsymbol{\tau}}_r\boldsymbol{\tau}_t - \mu_i\tilde{\boldsymbol{\tau}}_t\dot{\boldsymbol{\tau}}_r + \mu_i\tilde{\boldsymbol{\tau}}_r\dot{\boldsymbol{\tau}}_t). \end{aligned} \tag{21}$$

Here, the matrix $\mathbf{U} = \mathbf{I} + \mu_i\tilde{\boldsymbol{\Omega}}_0^{\mathrm{T}}$ comprises the effect of the internal damping, and has a deciding effect on the stability.

The equations of motion of a shaft presented above, reduce in the linear case to the equations which were considered e.g., in references [3, 8]. A different form of these equations (see e.g., references [5, 6]) can be obtained when one makes use in the analysis of the displacement vector measured, as the generalized forces, in the co-ordinate system which rotates with the angular velocity $\boldsymbol{\Omega}_0$ relative to the inertial frame. These equations include additional non-linear terms, mainly of inertial character, due to the fact that in this case the displacements are measured in a moving frame. On the contrary, in this case one obtains

simpler expressions for the internal moments and torques. Also, for this model one can reduce the analysis of steady vibration to the study of equilibrium state. Below, a comparison with the results obtained in references [5, 6] will be included, thus verifying the model used in the present approach.

2.3. MATRIX EQUATION OF MOTION

Equation (19) and (21) supplemented by relations (15) and (16) describe a geometrically exact model of a rotating shaft. In this form, this is a system of partial differential equations of the first order with respect to the natural co-ordinate and of the second order with respect to time. Most of the non-linearities which appear in these equations are quadratic forms of the components of the vectors $\mathbf{u}$, $\boldsymbol{\phi}$, $\mathbf{N}$, $\mathbf{M}$. For example, the non-linear terms include the expressions $\tilde{\boldsymbol{\varepsilon}}_r\mathbf{n}$, $\tilde{\boldsymbol{\varepsilon}}_r\mathbf{m}$ which describe the non-linear curvature effects, the expression $\tilde{\boldsymbol{\varepsilon}}_t\mathbf{n}$ which is a result of using the Timoshenko model or the gyroscopic non-linearity $\tilde{\boldsymbol{\omega}}\mathbf{B}_2\boldsymbol{\omega}$. This last non-linear term is important in the analysis of coupled flexural and torsional vibrations. Also, the rotation matrix $\boldsymbol{\Phi}$ used here after Argyris [26] has been described by an expression which is close to a quadratic form. This matrix can be approximated as

$$\boldsymbol{\Phi} = \mathbf{I} + \tilde{\boldsymbol{\phi}} + \tfrac{1}{2}\tilde{\boldsymbol{\phi}}^2. \tag{22}$$

The vector $\boldsymbol{\tau}_r$, which describes the influence of the curvature and which depends on the matrix $\boldsymbol{\Phi}$, can be expressed in the form

$$\boldsymbol{\tau}_r = (\mathbf{I} - \tfrac{1}{2}\tilde{\boldsymbol{\phi}})\boldsymbol{\phi}'. \tag{23}$$

Similarly, one can approximate the vector $\boldsymbol{\tau}_t$ to

$$\boldsymbol{\tau}_t = (\mathbf{I} - \tilde{\boldsymbol{\phi}})\mathbf{u}' + \tilde{\mathbf{e}}_1\boldsymbol{\phi} - \tfrac{1}{2}\tilde{\boldsymbol{\phi}}\,\tilde{\mathbf{e}}_1\boldsymbol{\phi}. \tag{24}$$

The above discussion suggests that one can consider a simplified model in which all the non-linearities of the second order are preserved [27]. In comparison with the equations most frequently used, which are derived by energy methods, the present approach corresponds to preserving also the terms of the third order. Even though it is possible to reduce the present set of equation to the usual form, this reduction is not convenient due to the proposed analysis method. The possibility of writing the simplified set of equations used by the present author in the form of a one-matrix equation is shown below. This form facilitates the description of the analysis method and more importantly the preparation of the numerical algorithm. To show how the system can be reduced to a one-matrix equation one introduces the extended state vector $\mathbf{x}$ of dimension $N = 12$, made up of the three-dimensional vectors of generalized displacements and internal forces

$$\mathbf{x}^{\mathrm{T}} = [\boldsymbol{\zeta}_1^{\mathrm{T}}, \boldsymbol{\zeta}_2^{\mathrm{T}}, \boldsymbol{\zeta}_3^{\mathrm{T}}, \boldsymbol{\zeta}_4^{\mathrm{T}}] = [\mathbf{u}^{\mathrm{T}}, \boldsymbol{\phi}^{\mathrm{T}}, \mathbf{N}^{\mathrm{T}}, \mathbf{M}^{\mathrm{T}}]. \tag{25}$$

After using the discussed simplifications, all non-linear terms which appear in the equations of motion can be expressed by two non-linear vector functions. These functions depend on the components of the state vector (or their derivatives) and are defined as

$$\mathbf{f}(\mathbf{P}, \boldsymbol{\zeta}_\alpha, \boldsymbol{\zeta}_\beta) = \tilde{\boldsymbol{\zeta}}_\alpha\mathbf{P}\boldsymbol{\zeta}_\beta = \sum_{k=1}^{3} [\tilde{\mathbf{e}}_k^{\mathrm{T}} \otimes (\mathbf{e}_k^{\mathrm{T}}\mathbf{P})]\,(\boldsymbol{\zeta}_\alpha \otimes \boldsymbol{\zeta}_\beta),$$

$$\mathbf{g}(\mathbf{P}, \boldsymbol{\zeta}_\alpha, \boldsymbol{\zeta}_\beta) = \mathbf{e}_1\boldsymbol{\zeta}_\alpha^{\mathrm{T}}\mathbf{P}\boldsymbol{\zeta}_\beta = \sum_{k=1}^{3} [(\mathbf{e}_1\,\mathbf{e}_k^{\mathrm{T}}) \otimes (\mathbf{e}_k^{\mathrm{T}}\mathbf{P})]\,(\boldsymbol{\zeta}_\alpha \otimes \boldsymbol{\zeta}_\beta). \tag{26}$$

Here $\mathbf{e}_k$ is a unit vector of dimension 3. In writing formulae (26) the Kronecker product of two matrices has been used [13]. The Kronecker product notation proves useful not only in the transformation of the equations of motion but also for their discretization discussed later on in the paper. In the general case of arbitrary matrices $\mathbf{A}$ and $\mathbf{B}$, the Kronecker product $\mathbf{A} \otimes \mathbf{B}$ can be defined as a supermatrix in which the ijth submatrix is $A_{ij}\mathbf{B}$.

The constant matrix $\mathbf{P}$ appearing in relations (26) has components which depend on the parameters of the system. Its detailed form depends on the non-linear term being considered. For example, after simplifying the non-linearity $\tilde{\boldsymbol{\varepsilon}}_r \mathbf{n}$ to the quadratic form one obtains the term $\tilde{\boldsymbol{\phi}}' \mathbf{N} = \mathbf{f}(\mathbf{I}, \boldsymbol{\zeta}'_2, \boldsymbol{\zeta}_3)$, when for the non-linearity $\mathbf{e}_1 \boldsymbol{\tau}_r^{\mathrm{T}} \mathbf{J}_0^t \dot{\boldsymbol{\tau}}_r$ appearing in equation (21) one obtains in a similar way the term $\mathbf{e}_1 \boldsymbol{\phi}'^{\mathrm{T}} \mathbf{J}_0^t \dot{\boldsymbol{\phi}}' = \mathbf{g}(\mathbf{J}_0^t, \boldsymbol{\zeta}'_2, \dot{\boldsymbol{\zeta}}'_2)$.

In order to reduce equations (15), (19) and (21) to the one-matrix equation one needs to use the identity

$$\boldsymbol{\zeta}_\alpha \otimes \boldsymbol{\zeta}_\beta = \boldsymbol{\vartheta}_{\alpha\beta}(\mathbf{x} \otimes \mathbf{x}). \tag{27}$$

The rectangular matrices $\boldsymbol{\vartheta}_{\alpha\beta}$ ($\alpha, \beta = 1, \ldots, 4$) with dimension $(3^2 \times 12^2)$ have a relatively simple form. For given values of the indices α, β the only non-zero elements of the matrices $\boldsymbol{\vartheta}_{\alpha\beta}$, which are all equal to one, are given by the indices

$$p = 3(m-1) + n, \qquad q = 36(\alpha - 1) + 12(m-1) + 3(\beta - 1) + n, \tag{28}$$

where m, n change within (1–3). Now, equations (26) can be written as

$$\mathbf{f}(\mathbf{P}, \boldsymbol{\zeta}_\alpha, \boldsymbol{\zeta}_\beta) = \mathbf{f}_{\alpha\beta}(\mathbf{P})(\mathbf{x} \otimes \mathbf{x}), \qquad \mathbf{g}(\mathbf{P}, \boldsymbol{\zeta}_\alpha, \boldsymbol{\zeta}_\beta) = \mathbf{g}_{\alpha\beta}(\mathbf{P})(\mathbf{x} \otimes \mathbf{x}). \tag{29}$$

The (3×12^2) rectangular matrices $\mathbf{f}_{\alpha\beta}$, $\mathbf{g}_{\alpha\beta}$ are defined as

$$\mathbf{f}_{\alpha\beta}(\mathbf{P}) = \sum_{k=1}^{3} [\tilde{\mathbf{e}}_k^{\mathrm{T}} \otimes (\mathbf{e}_k^{\mathrm{T}} \mathbf{P})]\, \boldsymbol{\vartheta}_{\alpha\beta}, \qquad \mathbf{g}_{\alpha\beta}(\mathbf{P}) = \sum_{k=1}^{3} [(\mathbf{e}_1 \mathbf{e}_k^{\mathrm{T}}) \otimes (\mathbf{e}_k^{\mathrm{T}} \mathbf{P})]\, \boldsymbol{\vartheta}_{\alpha\beta}. \tag{30}$$

Finally, the equations of motion can be written in the form of a matrix partial differential equation as

$$\sum_{i=0}^{1} \sum_{k=0}^{2} \mathbf{A}_k^i \frac{\partial^{i+k} \mathbf{x}}{\partial s^i \partial t^k} + \sum_{i,j=0}^{1} \sum_{k,l=0}^{2} \mathbf{F}_{kl}^{ij} \left(\frac{\partial^{i+k} \mathbf{x}}{\partial s^i \partial t^k} \otimes \frac{\partial^{j+l} \mathbf{x}}{\partial s^j \partial t^l} \right) = \mathbf{0}. \tag{31}$$

Here $i, j = 0, 1$ (the system is of the first order with respect to the natural co-ordinate s) and $k, l = 0, 1, 2$ (second order with respect to time).

The determination of the square matrices $\mathbf{A}_k^i$ $(N \times N)$, which describe the linear term, does not cause problems. The rectangular matrices $\mathbf{F}_{kl}^{ij}$ $(N \times N^2)$, which account for the geometric non-linearities, can be expressed through matrices (30). The formulae for the non-zero matrices $\mathbf{A}_k^i$ and $\mathbf{F}_{kl}^{ij}$ are provided in Appendix A. Form (31) of the equations of motion helps considerably in the presentation of the analytical method and of the construction of a suitable algorithm for numerical calculations.

3. THE GALERKIN METHOD

A method of discretization which allows reduction of the solution of the non-linear partial differential matrix equation (31) to the solution of a non-linear algebraic equation is discussed below. This algebraic equation will be called the matrix equation of amplitudes. The approach is based on the Galerkin method, and the equations are first discretized in the space domain followed by the time discretization. In discussing the space discretization, no

special form of the shape functions is assumed. However, in order not to complicate the presentation too much, the same shape functions are assumed for all the components of the shape vector. Other discretization methods have also been used for comparison, and the results discussed in the present paper were found to agree with those obtained using the Rayleigh–Ritz method. It has been found that the Galerkin method applied to the space formulation is much less sensitive (e.g., to the shear-locking problem) than the methods (e.g., the Rayleigh–Ritz method) in which only the approximation of displacements and rotation angles is used. In all numerical calculations one uses the polynomial B-spline functions discussed e.g., in reference [28].

3.1. SPATIAL DISCRETIZATION

One seeks the solution of equation (31) in the form

$$\mathbf{x}(s,t) = \mathbf{V}^{\mathrm{T}}(s)\mathbf{y}(t), \qquad \mathbf{V}^{\mathrm{T}}(s) = \mathbf{I}_{(N)} \otimes \mathbf{v}(s)^{\mathrm{T}}. \tag{32}$$

Here, $\mathbf{v}(s)$ is a vector of the approximation functions with dimension M and $\mathbf{I}_{(N)}$ is a unit matrix of dimension N. To obtain the discretized equations of motion, the Galerkin method is used. To this end, one multiplies the left side of equation (31) by the matrix $\mathbf{V}$, and integrates the result in the interval $(0, l)$. To avoid the necessity of integrating at each step of the iteration method, it is necessary to make additional transformations to the equation so obtained. For this, the identity

$$\mathbf{V}\mathbf{A}_k^i\mathbf{V}_i^{\mathrm{T}} = \mathbf{A}_k^i \otimes (\mathbf{v}\mathbf{v}_i^{\mathrm{T}}) \tag{33}$$

is useful, where $\mathbf{v}_0 = \mathbf{v}(s)$, $\mathbf{v}_1 = \mathbf{v}'(s)$. One can also show that

$$\mathbf{V}\mathbf{F}_{kl}^{ij}(\mathbf{V}_i^{\mathrm{T}} \otimes \mathbf{V}_j^{\mathrm{T}}) = [\mathbf{F}_{kl}^{ij} \otimes (\mathbf{v}_i^{\mathrm{T}} \otimes \mathbf{v}\mathbf{v}_j^{\mathrm{T}})]\,\boldsymbol{\Delta}(N, M), \tag{34}$$

where matrix $\boldsymbol{\Delta}$ is defined as

$$\boldsymbol{\Delta}(N, M) = \sum_{m=1}^{M} \mathbf{I}_{(N)} \otimes \mathbf{e}_{(M)m}^{\mathrm{T}} \otimes \mathbf{I}_{(N)} \otimes \mathbf{e}_{(M)m} \otimes \mathbf{I}_{(M)}. \tag{35}$$

In equation (35), $\mathbf{e}_{(M)m}\,(m = 1, \ldots, M)$ is a system of unit vectors of dimension M, whereas $\mathbf{I}_{(N)}$ and $\mathbf{I}_{(M)}$ are the unit matrices of the respective dimension. In spite of the apparently complex form of matrix $\boldsymbol{\Delta}$ which has dimension $(N^2M^2 \times N^2M^2)$, each of its rows has only one non-zero element, which is equal to 1. The elements of matrix $\boldsymbol{\Delta}$ can be written in the form

$$\boldsymbol{\Delta}_{nm} = \delta_{i_1}^{i_2}\delta_{j_1}^{j_2}\delta_{k_1}^{k_2}\delta_{l_1}^{l_2}, \tag{36}$$

where

$$\begin{aligned} n &= (i_1 - 1)M^2N + (j_1 - 1)M^2 + (k_1 - 1)M + l_1, \\ m &= (i_2 - 1)M^2N + (k_2 - 1)MN + (j_2 - 1)M + l_2. \end{aligned} \tag{37}$$

In formulae (36) and (37) the indices i_1, i_2, j_1, j_2 assume values from within the range $(1, \ldots, N)$, and k_1, k_2, l_1, l_2 have values from $(1, \ldots, M)$. Due to the form of the $\boldsymbol{\Delta}$ matrix, the multiplication of an arbitrary matrix $\mathbf{A}$ by $\boldsymbol{\Delta}$ results in the interchange of the corresponding columns, according to the scheme $[\mathbf{A}\boldsymbol{\Delta}]_{lm} = \sum_{n=1}^{N^2M^2} A_{ln}\Delta_{nm} = A_{ln(m)}$, where $n(m)$ can be

easily calculated, especially numerically, by substituting into relations (37) $i_1 = i_2, j_1 = j_2$, $k_1 = k_2$ and $l_1 = l_2$ in the respective ranges. Now if one introduces the notation

$$\boldsymbol{\Upsilon}_i = \int_0^l \mathbf{v}(s)\,\mathbf{v}_i^{\mathrm{T}}(s)\,\mathrm{d}s, \qquad \boldsymbol{\Upsilon}_{ij} = \int_0^l \mathbf{v}_i^{\mathrm{T}}(s) \otimes \mathbf{v}(s)\,\mathbf{v}_j^{\mathrm{T}}(s)\,\mathrm{d}s, \tag{38}$$

one can write the resulting system of ordinary time differential equations in the form

$$\sum_{k=0}^{2} \mathbf{A}_k \frac{\mathrm{d}^k \mathbf{y}}{\mathrm{d}t^k} + \sum_{k,l=0}^{2} \mathbf{F}_{kl}\left(\frac{\mathrm{d}^k \mathbf{y}}{\mathrm{d}t^k} \otimes \frac{\mathrm{d}^l \mathbf{y}}{\mathrm{d}t^l}\right) = \mathbf{0}. \tag{39}$$

Here

$$\mathbf{A}_k = \sum_{i=0}^{1} \mathbf{A}_k^i \otimes \boldsymbol{\Upsilon}_i, \qquad \mathbf{F}_{kl} = \sum_{i,j=0}^{1} (\mathbf{F}_{kl}^{ij} \otimes \boldsymbol{\Upsilon}_{ij})\,\boldsymbol{\Delta}(N, M). \tag{40}$$

The dimensions of the square matrices $\mathbf{A}_k$ as well as the rectangular $\mathbf{F}_{kl}$ are now given by the product NM, where N is the dimension of the state vector $\mathbf{x}$ and M is the dimension of the shape function vector.

3.2. TIME DISCRETIZATION

One repeats the Galerkin method for the system of equations (39) by assuming the approximate solution in a form similar to equation (32)

$$\mathbf{y}(t) = \mathbf{W}^{\mathrm{T}}(t)\,\mathbf{a}, \qquad \mathbf{W}^{\mathrm{T}}(t) = \mathbf{I}_{(NM)} \otimes \mathbf{w}(t)^{\mathrm{T}}. \tag{41}$$

In studying steady state vibrations, e.g., steady state undamped or self-excited vibration, one can assume the components of the $\mathbf{w}$ vector of dimension $L = 2K + 1$ in the form of periodic functions $\cos k\omega t$, $\sin k\omega t$. Due to the non-symmetric, in general, character of vibration it is necessary to also include a constant term (e.g., constant components of axial forces). One assumes the approximate solution in the form

$$\mathbf{w}^{\mathrm{T}}(t) = [1, \cos\omega t, \cos 2\omega t, \ldots, \cos K\omega t, \sin\omega t, \ldots, \sin K\omega t]. \tag{42}$$

In applying the Galerkin method it is necessary to calculate the integrals

$$\boldsymbol{\Theta}_k = \int_0^{\mathrm{T}} \mathbf{w} \frac{\mathrm{d}^k \mathbf{w}^{\mathrm{T}}}{\mathrm{d}t^k}\,\mathrm{d}t, \qquad \boldsymbol{\Theta}_{kl} = \int_0^{\mathrm{T}} \frac{\mathrm{d}^k \mathbf{w}^{\mathrm{T}}}{\mathrm{d}t^k} \otimes \mathbf{w} \frac{\mathrm{d}^l \mathbf{w}^{\mathrm{T}}}{\mathrm{d}t^l}\,\mathrm{d}t. \tag{43}$$

Moreover, one can use the following relations, which are a result of the assumed solution (42):

$$\mathrm{d}^k \mathbf{w}^{\mathrm{T}}/\mathrm{d}t^k = \mathbf{w}^{\mathrm{T}} \boldsymbol{\Gamma}^k \omega^k. \tag{44}$$

The matrix $\boldsymbol{\Gamma}$ has the form

$$\boldsymbol{\Gamma} = \begin{bmatrix} \mathbf{0} & \mathbf{T} \\ -\mathbf{T} & \mathbf{0} \end{bmatrix} \tag{45}$$

and the elements of the matrix $\mathbf{T}$ are given by the formula

$$\mathbf{T}_{nm} = (n-1)\,\delta_{n-1}^{m}, \quad n = 1, \ldots, K+1, \quad m = 1, \ldots, K. \tag{46}$$

Equations (43) can now be written in the form

$$\mathbf{\Theta}_k = \mathbf{\Theta}_0 \mathbf{\Gamma}^k \omega^k, \qquad \mathbf{\Theta}_{kl} = \mathbf{\Theta}_{00}(\mathbf{\Gamma}^k \otimes \mathbf{\Gamma}^l)\omega^{k+l}. \tag{47}$$

Therefore, one has only to calculate matrices $\mathbf{\Theta}_0$ and $\mathbf{\Theta}_{00}$. Since $\mathbf{\Theta}_0$ is a diagonal matrix of dimension $(L \times L)$, one can trivially calculate the inverse of this matrix. The matrix $\mathbf{\Theta}_{00}$ is rectangular and has dimension $(L \times L^2)$. After applying the Galerkin method one obtains a system of equations, which upon multiplication from left by the matrix $\mathbf{I}_{(NM)} \otimes (\mathbf{\Theta}_0)^{-1}$, can be reduced to the form

$$\mathbf{g}(\mathbf{a}, \omega) = \mathbf{A}(\omega)\mathbf{a} + \mathbf{F}(\omega)(\mathbf{a} \otimes \mathbf{a}) = \mathbf{0}, \tag{48}$$

Here, the notation

$$\mathbf{A} = \sum_{k=0}^{2} \mathbf{A}_k \otimes \mathbf{\Gamma}^k \omega^k, \qquad \mathbf{F} = \sum_{k,l=0}^{2} [\mathbf{F}_{kl} \otimes \mathbf{\Theta}(\mathbf{\Gamma}^k \otimes \mathbf{\Gamma}^l)]\, \mathbf{\Delta}(NM, L)\omega^{k+l} \tag{49}$$

is used in which

$$\mathbf{\Theta} = (\mathbf{\Theta}_0)^{-1} \mathbf{\Theta}_{00}. \tag{50}$$

Equation (48) is called the matrix equation of amplitudes. It gives a relation between the amplitude vector $\mathbf{a}$ and the frequency ω. The main advantage of this equation is the fact that the matrices $\mathbf{A}$ and $\mathbf{F}$ defined by formulae (40) and (49) do not depend on the state vector co-ordinates. They are expressed by Kronecker products of matrices $\mathbf{A}_k^i$, $\mathbf{F}_{kl}^{ij}$ depending only on the parameters of the investigated system and the matrices $\mathbf{\Upsilon}_i$, $\mathbf{\Upsilon}_{ij}$,$\mathbf{\Theta}_k$, $\mathbf{\Theta}_{kl}$, which depend on the assumed approximating functions. For some qualitative investigations, at the beginning of the iterative process of solution of non-linear problem (48), the values of corresponding integrals (38) and (43) can be predicted. By this approach the application of the Galerkin method leads practically to the prediction of the Kronecker products of already known matrices. It allows considerable reduction in the time of numerical calculations.

3.3. SOLUTION OF MATRIX AMPLITUDE EQUATION

The general form of the non-linear problem (48), which uses the definition of the Kronecker product of two matrices to write the non-linear terms, is very convenient in the numerical analysis. Based on form (48), one can easily calculate the tangent matrix, which is given by

$$\mathbf{g}_a = \mathbf{A} + \mathbf{F}(\mathbf{a} \otimes \mathbf{I}_{(S)} + \mathbf{I}_{(S)} \otimes \mathbf{a}), \tag{51}$$

where $S = NML$. The tangent matrix (51) is used in the Newton–Raphson method. In a similarly simple way one can calculate the Hessian matrix of second derivatives given by a rectangular matrix $\mathbf{g}_{aa} = 2\mathbf{F}$. In the analysis of the free vibration problem it is convenient, based on formula (49), to group the terms of the $\mathbf{A}$ matrix for different powers of ω. It allows determination of the vector $\mathbf{g}_\omega$ which is the derivative of equation (48) with respect to the parameter ω used in the sequel to find the bifurcation points.

To solve the non-linear problem (48) iterative continuation methods are usually used where the next point of some characteristics of the system is predicted on the basis of the solution at previous point. To this end, it is convenient to supplement an additional

constraint equation (parameterizing equation (see, e.g., references [15, 20]). In the calculations presented below, applying the method based on the increment of the arc length as the control parameter, the following form of equation proposed by Crisfield [29] is used

$$h(\mathbf{a}) = \Delta\mathbf{a}^{\mathrm{T}}\Delta\mathbf{a} - (\Delta\alpha)^2 = 0. \tag{52}$$

Here $\Delta\mathbf{a} = \mathbf{a}^i - \mathbf{a}^{i-1}$ is the increment of the amplitude vector between two points lying on the determined characteristics.

To this end it is noted that the systems described in the paper are autonomous. To eliminate the ambiguous solutions the initial phase was fixed on the basis of the phase condition (see, e.g., reference [14]). This condition can be easily realized by comparing to zero one of the components of the vector of amplitudes. Applying the continuation methods, the so-called primary path (or first main branch) can be predicted. Their graphical illustration, in case of free vibration, are the so-called backbone curves. To this end, the primary bifurcation points, which are the solution of the linear problem connected with the non-linear one, should be predicted. The suitable normalized solution of the linear problem can be taken as the start solution in the continuation method. By investigation of the internal resonance phenomenon the additional paths of solutions (so-called post-bifurcation paths or secondary branches) starting at the secondary bifurcation points should be predicted. To find the secondary bifurcation points the sign of the determinant of the tangent matrix was checked. At the critical points $\det \mathbf{g}_a(\mathbf{a}^*, \omega^*) = 0$ to distinguish the bifurcation and limit points, the following condition was checked (see, e.g., reference [12]):

$$\mathbf{g}_\omega^{\mathrm{T}}\boldsymbol{\varphi} = 0. \tag{53}$$

Here, $\boldsymbol{\varphi}$ is the eigenmode corresponding to the zero eigenvalue of the matrix $\mathbf{g}_a$. If condition (53) is not satisfied at a critical point, this is a limit point and to find the next point on the curve one can use the Newton method.

To find the post-bifurcation branch, one uses the vector $\boldsymbol{\varphi}$, which is conveniently normalized from the condition $\|\boldsymbol{\varphi}\| = \|\mathbf{a}^*\|$. One can then look for the first approximation as

$$\omega_1^i = \omega^*, \qquad \mathbf{a}_1^i = \mathbf{a}^* + \mu\boldsymbol{\varphi}. \tag{54}$$

From the numerical simulations it has been found that good convergence is achieved taking the coefficient μ from within the range (0·01–0·1).

4. NUMERICAL EXAMPLES

The non-linear shaft model presented above and the proposed method of analysis were applied to the investigation of self-excited vibration and the internal resonance phenomenon. To present the results of numerical analysis, non-dimensional quantities were used by dividing the amplitudes by the radius of inertia (α) of the cross-section, and giving the frequency relative to the lowest frequency ω_1 of a shaft in the absence of rotation ($v = \omega/\omega_1$). The parameter $\beta = l/r$ (where l is the length and $2r$ the diameter of the shaft) denotes the shaft slenderness.

4.1. INTERNAL RESONANCE

In the paper by Leung and Fung [19] the phenomenon of internal resonance was shown for the case of hinged–clamped (type 1:3) and clamped–clamped beams (type 1:5).

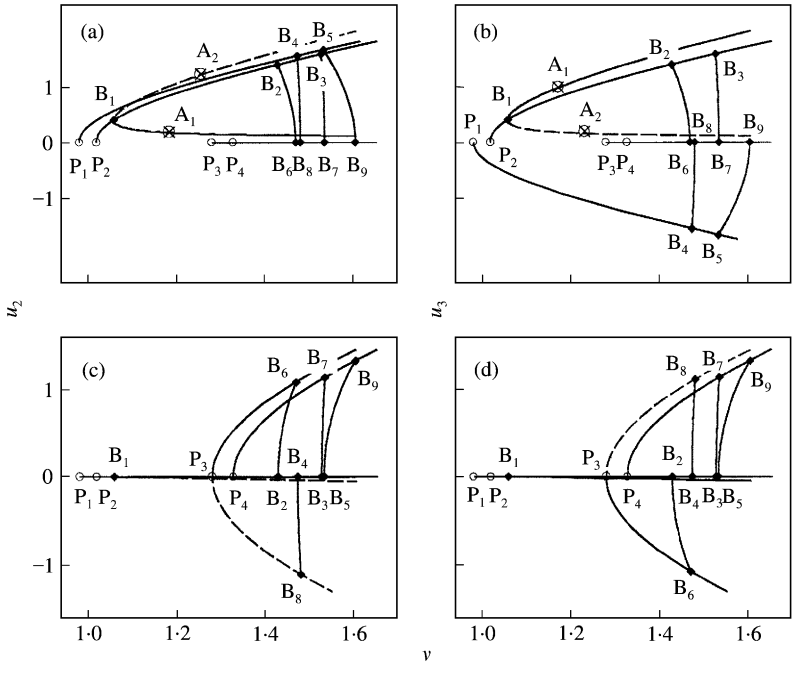

Figure 2. Backbone curves of simply supported shaft for $\beta = 25$ and $\eta = 5$: (a) first harmonic u_2; (b) first harmonic u_3; (c) third harmonic u_2; (d) third harmonic u_3.

Lewandowski studied, in references [12, 30], internal resonance in single-span and multiple-span simply supported beams. This is done despite the fact that the analysis of the vibration of beams, as well as a system more related to the present study as described in reference [31] consisted of a cantilever beam attached to a rotating body suggesting the possibility of internal resonance appearing in these kind of systems.

The chosen results of a numerical analysis, concerning the shaft simply supported with axially fixed ends, were presented. In Figure 2, the dynamical characteristics for the first and third harmonics of the transverse displacements in two perpendicular directions u_2 and u_3 at the fixed point $s = l/4$ with $\beta = 25$ and $\eta = \Omega_0/\omega_1 = 5$ are shown. The plots shown in Figure 2 were obtained by approximation of the displacements in the direction by the cosine series and those in the other direction by the sine series, which is a consequence of the assumed phase condition. Therefore, the curves with different signs of the "amplitudes" (curve P_1B_4—see Figures 2(a) and 2(b), curve P_3B_8—Figures 2(c) and 2(d)) can be interpreted as the characteristics of the backward modes, whereas the curves with positive "amplitudes" (curves P_2B_2, P_4B_7) are related to the forward modes.

The symbols P_j are used to denote the primary bifurcation points, whereas the secondary bifurcation points are denoted as B_j. Here, the curves with the origin at points P_1 and P_2 are the primary paths, whereas the curves starting points P_3 and P_4 are the subharmonic curves of the next non-symmetric vibration modes. The points P_3 and P_4 are determined by the suitable submultiples of the third and fourth eigenfrequencies. The subharmonic branches play a role in the explanation of the internal resonance phenomenon.

By analyzing the matrix equation of amplitudes it is possible to predict the secondary bifurcation points using the corresponding condition for the tangent matrix. It is shown that on the path related to the forward mode there are three bifurcation points B_1, B_2 and B_3. On the path related to the backward mode there are two bifurcation points, B_4 and B_5.

These calculated points are the start points for the post-bifurcation paths illustrating the process of modes changes during the internal resonance phenomenon.

At the first bifurcation point B_1 the primary path P_2B_1 intersects the post-bifurcation path $A_1B_1A_2$. The curve $A_1B_1A_2$ is, despite the apparent similarity, different for the displacements u_2 and u_3. When the amplitude of the displacements falls off with frequency in one direction it increases in the other direction (the continuous lines) and *vice versa* (the dashed line). An interesting phenomenon takes place in which the forward and backward modes are excited with the same frequency. This phenomenon could be termed as the internal resonance of type 1:1, even though in this case there in no visible transformation of the forward mode of vibration into the backward one. An arbitrary point on the shaft axis moves in this case on an ellipsis.

It should be pointed out that a similar mode of vibration which is a superposition of the forward and backward modes is also possible in a linear system, but due to the fact that the frequencies of the two modes are slightly different, the trajectory of a point on the shaft axis is an ellipsis which lies in a plane rotating relative to the fixed frame. Moreover, the velocity at which the plane rotates is equal to the difference of the frequencies of the forward and backward modes. As a result, in the fixed frame one can observe the characteristics beat pattern.

Except secondary bifurcation points B_1–B_5, stepping out on primary paths, one can detect additional bifurcation points B_6–B_9 lying on post-bifurcation paths and belonging simultaneously to suitable subharmonic branches.

The curve B_2B_6 illustrates the behavior of the system with three-times higher frequency. Lying on this curve is the bifurcation point B_6, through which passes the subharmonic curve P_3B_6. The curve P_3B_6 begins at point $v = v_3/3$, where v_3 is the non-dimensional frequency of the linear system corresponding to the non-symmetric mode of backward precession. At point B_6 the internal resonance of type 1:3 between the symmetric forward and non-symmetric backward modes takes place and some analogy to the behavior of simply supported beams discussed in reference [30] can be observed.

The post-bifurcation curve B_3B_7 illustrates the behavior of the system in going from the symmetric forward mode to the non-symmetric forward mode.

The secondary branches B_4B_8 and B_5B_9 describe the internal resonance between the symmetric and non-symmetric backward modes and between the symmetric backward and non-symmetric forward modes.

The variation of the parameters β and η do not cause the qualitative changes of the characteristics of the system investigated. Increasing the coefficient β and decreasing the value of the rotation speed η decreases the difference between values of frequency at the points B_k for $k = 2, 3, 4, 5$. To illustrate the influence of the parameters β and η the values of frequency at the discussed bifurcation points obtained for the Euler- and Timoshenko-type models are given in Table 1. For $\eta = 0$ (beam) all the values are the same (point B_0). It is

TABLE 1

The values of non-dimensional frequencies at the bifurcation points

Model of the system	Reference [30] Beam $\eta = 0$	Reference [32]	Present analysis				
				Shaft $\eta = 5$			
	B_0	B_0	B_0	B_2	B_3	B_4	B_5
EM	1·446–1·451	1·439–1·442	1·444	1·544	1·550	1·546	1·552
TM	—	—	1·390	1·440	1·497	1·474	1·552

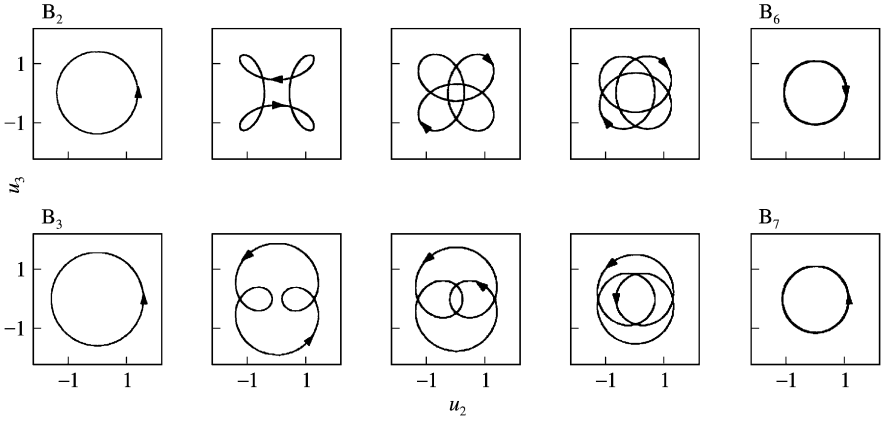

Figure 3. Periodic orbits at point $s = l/4$; paths B_2B_6 and B_3B_7.

possible to compare the present results with the results obtained in references [30, 32] for the Euler-type beam with circular and rectangular cross-sections. In these cited works, the frequency range with the bifurcation point was given.

It is very interesting to consider the trajectories of an arbitrary point on the shaft (e.g., point $s = l/4$) corresponding to the points on the post-bifurcation paths. They illustrate the process of changing of the vibration modes. These trajectories, which are shown in Figure 3 (for the paths B_2B_6 and B_3B_7), were found by the numerical integration of the ordinary differential equations (39) obtained after spatial discretization. The corresponding initial conditions have been calculated by the approximate method using the matrix equation of amplitudes. A very good repeatability of the trajectories (integration in time corresponding to 50 periods) is an additional proof of a good convergence of the approximate analysis. Trajectories corresponding to the points lying on the paths B_4B_8 and B_5B_9 are in qualitative substance very close to paths obtained for B_3B_7 and B_2B_6 respectively.

4.2. SELF-EXCITED VIBRATIONS

4.2.1. *Influence of the rotation speed*

In reference [5] Shaw and Shaw analyzed the influence of internal and external damping as well as the rotation speed on the amplitude of simply supported shaft modelled as an Euler beam. An analysis of the results of this study shows that two parameters considerably influence the stability regions and the characteristics of steady state vibrations of the system. The first is the non-dimensional coefficient $\gamma = \breve{\mu}_e/\breve{\mu}_i$, defined as the ratio of non-dimensional external damping coefficient $\breve{\mu}_e = \mu_e/\rho A\omega_1$ to non-dimensional coefficient of internal damping $\breve{\mu}_i = \mu_i\omega_1$. Here ρA is the mass per unit length of the shaft. The second parameter is the ratio $\eta = \Omega_0/\omega_1$ of the rotation speed to the lowest frequency of the shaft at rest. In studying the limit cycles corresponding to higher modes of vibration, it is convenient to use parameters γ_n and η_n, defined in a similar way, with respect to the nth frequency ω_n of the linear system.

It has been proved in reference [5] for a simplified shaft model, that in the absence of external damping ($\mu_e = 0$), for $\eta_n > 1$ synchronous vibration is excited ($v = \omega/\Omega_0 = 1$) and that the amplitude of vibration defined as the maximum displacement value is independent

TABLE 2

Amplitudes of self-excited oscillations of a simply supported shaft

	Reference [5]			Present analysis					
	Euler model			$\beta = 500$			$\beta = 25$		
Mode	$\eta = 2$	$\eta = 5$	$\eta = 10$	$\eta = 2$	$\eta = 5$	$\eta = 10$	$\eta = 2$	$\eta = 5$	$\eta = 10$
First	3·464	9·798	19·900	3·465	9·798	19·902	3·416	4·465	4·475
Second	—	1·500	4·583	—	1·500	4·582	—	1·485	2·337
Third	—	—	0·969	—	—	0·969	—	—	1·036

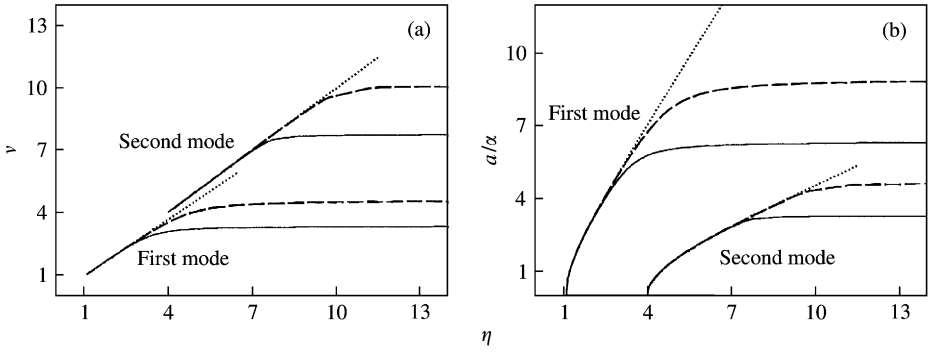

Figure 4. Influence of the rotation speed for simply supported shaft: (a) frequency; (b) amplitude. Key: ····, Euler model; - - - -, $\beta = 100$; ——, $\beta = 50$.

of the magnitude of internal damping. The value of the amplitude relative to the shaft radius of inertia α is given by the simple formula

$$a_n/\alpha = 2\sqrt{\eta_n^2 - 1}. \tag{55}$$

This case ($\gamma = 0$) is used as a benchmark solution to test the convergence of the present method. The amplitudes have been calculated for three different values of the rotation speed choosing the values of parameter η such that one, two or three modes of self-excited oscillation are exited. Results thus obtained are shown in Table 2.

The general model described by equations (19) and (21) has been used in the calculations, which accounts for the coupling between the flexural, longitudinal and torsional vibrations. The Euler case is obtained by increasing the value of the parameter β. The very good agreement for very large values of β with equation (55) verifies the model used and good convergence.

Considerable discrepancy of results is observed in the case of short shafts ($\beta = 25$), when the results obtained from the Timoshenko model are more realistic than those obtained on the basis of those analyzed in the reference [5] Euler model. These discrepancies are also visible in Figure 4, which shows the dependence of frequency and amplitude versus the rotation speed for the first (symmetric) and second (non-symmetric) vibration modes. The plots shown illustrate the behavior of the models, for different values of the parameters β (50, 100), for the established value of coefficient $\gamma = 0{\cdot}1$.

For rotation speeds which are only slightly above the critical value, the results from the simplified model [5] and those obtained using equations (19) and (21) are identical. The discrepancies for a given mode (e.g., the first mode) start to show in the range of the rotation speed which includes the next critical speed (second in Figure 4).

From the results obtained for the Euler model (the dotted lines), practically linear dependence of the frequency of vibration on the rotation speed is predicted, and the frequencies of the two modes being considered are very close for small values of the parameter γ. In the absence of external damping when the coefficient $\gamma = 0$, different modes of self-excited oscillations with the same frequency equal to the shaft rotation speed (the synchronous vibration) theoretically are possible. The non-dimensional value of the amplitude increases greatly with the increase of the rotation speed. Because the non-dimensional amplitude is related to the radius of inertia of the shaft cross-section, especially in the case of short shafts, large displacements can be excited in the process of self-excited vibration.

Different results are obtained in this range of the rotation speed by applying the Timoshenko model, but in this case it is also important to take into account the coupling between the flexural modes and the mostly torsional ones. For the rotation speed above the second critical speed ($\eta \approx 4$) the amplitude and frequency of the first vibration mode tends to settle down, as shown in Figure 4. For the rotation speed above the next critical speed ($\eta \approx 9$) the frequency and amplitude of the second vibration mode also tend to settle down. One can also observe important difference for models with different values of the parameter β—the non-dimensional amplitudes of short shafts ($\beta = 50$) are a little lower than in the case of slender shafts ($\beta = 100$).

In the explanation of the above results, there is an important contribution of the non-linear term $\tilde{\boldsymbol{\tau}}_r \mathbf{M}$, which appears in the second of equations (19), and which influences the torsional deformations of the shaft in the presence of internal damping (through matrix $\mathbf{U}$ in the second of equations (21)). This term has an interpretation of the cross-product of the vector $\boldsymbol{\tau}_r$ and the moment vector $\mathbf{M}$. When the effect of internal damping and the rotation speed can be neglected, the components of the moments vector depend linearly on the components of the vector $\boldsymbol{\tau}_r$. In this case the equation of the torsional vibration does not depend on the flexural displacements of the shaft.

4.2.2. *Influence of damping*

To illustrate the influence of damping Figure 5 shows the dependence of non-dimensional frequency of vibration on the parameter γ. The results shown explore the case of a simply supported shaft with the coefficient $\eta = 6$. For this value of the rotation speed two modes of the self-excited vibration can be excited. The values of frequency and amplitudes (not shown here) of vibration decrease when the values of parameter γ increases. This fact confirms the results obtained in reference [5]. The center manifold theory applied in the cited paper shows that both the limit cycles are stable. However, the authors pointed out that for the small values of the parameter γ the dominant unstable character of the first mode occured.

The accuracy of the solutions discussed above and their stability can be verified by performing the numerical integration of the system of differential equations (39). The results of these calculations depend on the initial conditions. On the basis of such numerical calculations, the ranges of the stable solutions were marked (Figure 5).

The solutions shown in Figures 6 and 7 were obtained by assuming two different variants of initial conditions. In the first variant, zero displacements were assumed and the initial velocities were chosen in such a way as to easily excite the first or the second vibration mode. In the second case, the initial conditions were taken from the solutions obtained by

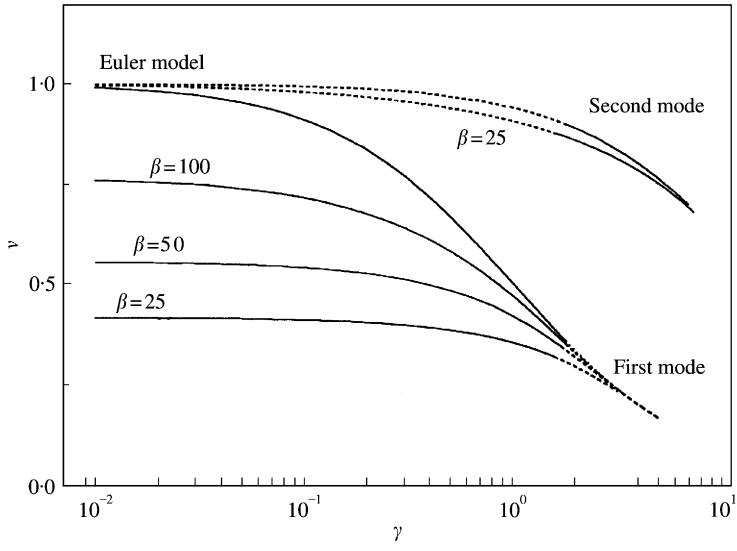

Figure 5. Influence of the parameter γ on the frequency of self-excited stable (——) and unstable (- - - -) vibration.

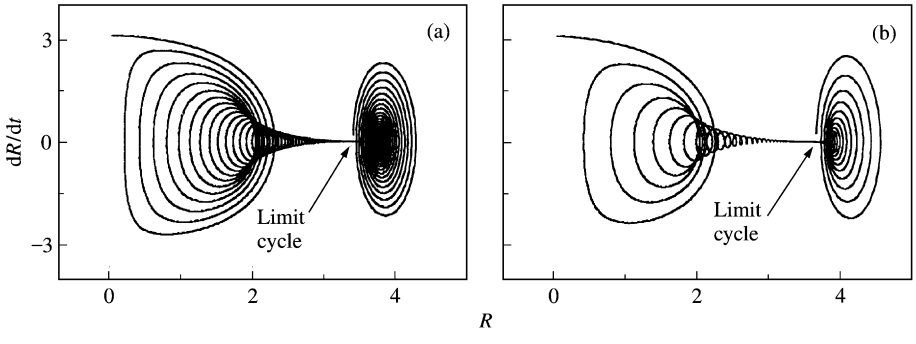

Figure 6. Influence of the co-efficients $\breve{\mu}_i$ and $\breve{\mu}_e$ on the phase trajectories for the first vibration mode: (a) $\breve{\mu}_i = \breve{\mu}_e = 0{\cdot}02$; (b) $\breve{\mu}_i = \breve{\mu}_e = 0{\cdot}04$.

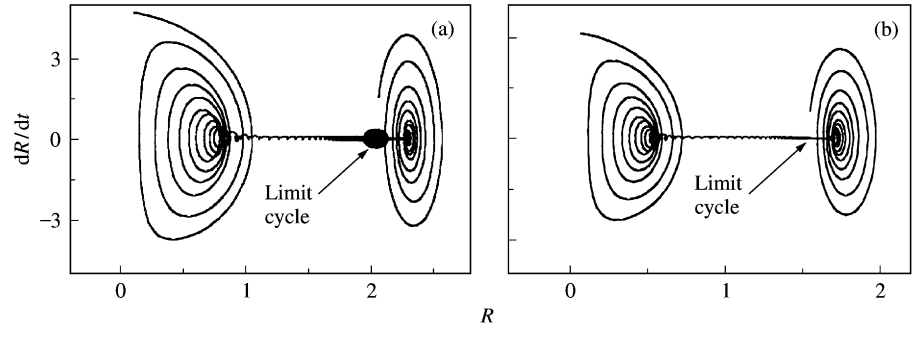

Figure 7. Influence of the parameters γ on the phase trajectories for the second vibration mode: (a) $\breve{\mu}_i = 0{\cdot}02$, $\breve{\mu}_e = 0{\cdot}002$; (b) $\breve{\mu}_i = 0{\cdot}02$, $\breve{\mu}_e = 0{\cdot}04$.

the method of analysis discussed above by proportionally increasing the velocities in one of the transverse directions. Both variants can be interpreted as applying a properly chosen impulsive excitation, which in the first variant acts on the undeformed shaft and in the second variant disturbs the steady state condition. In presenting the results the characteristics are limited to being shown at one point at a distance equal to 1/4 of the shaft axis from the end. This choice is motivated by the fact that the second mode of self-excited oscillations is antisymmetric for the type of boundary conditions in question and has a nodal point in the middle of the shaft.

Figures 6 and 7 show the phase portraits of the transverse displacement defined as the distance of the analyzed point from the undeformed axis of the shaft ($R^2 = u_2^2 + u_3^2$). Figure 6 illustrates the process of the setting of the first mode of self-excited vibration for a fixed value of the parameter $\gamma = 1$ and for two different values of the coefficient $\breve{\mu}_i = \breve{\mu}_e$ (0·02, 0·04). The phase trajectories converge to the point which agrees with the result obtained by the approximation method. The behaviour of the phase trajectories is influenced not only by the value of the coefficient γ, but the parameters $\breve{\mu}_i$ and $\breve{\mu}_e$ which have had no effect on the results up to this point. The values of the internal and external damping influence, in the first instance, the time of setting of the self-excited oscillations. For lower damping values the time necessary to reach the limit cycle becomes much longer. The precise determination by the method of direct integration of the amplitudes of the self-excited vibration takes much more time than by the approximation method.

For small values of the parameter γ the lowest mode is dominant, whereas for sufficiently high values of γ higher modes dominate. This conclusion is confirmed by the phase portraits shown in Figure 7, which concern the second mode of self-excited vibration, for two values of the γ and for fixed values of $\breve{\mu}_i = 0{\cdot}02$ and $\eta = 6$. For $\gamma = 2$ (Figure 7b) the phase trajectories tend for both types of initial conditions to the same point. The second mode of vibration is stable.

For $\gamma = 0{\cdot}1$ (Figure 7(a)), even though the initial conditions are chosen to favour the excitation of the second mode, the lowest mode sets in eventually. The phase trajectories have in this case very complex shapes. The shape of the initial phase of this process is shown in Figure 7(a) (showing the complete process of reaching the limit cycle would obscure the plot). The solution tends first to the value corresponding to the second non-symmetric mode of vibration. However, as time increases the effect of the symmetric mode becomes more and more visible, and finally (which is not shown in Figure 7(a)) steady state vibration with the first mode is established. For high values of the parameter γ the case is the opposite, and a higher possibility exists of producing higher vibration modes. The total process of establishing of the suitable mode of vibrations is visible in Figures 8(a) and 8(b). These figures show the time plots for $\gamma = 0{\cdot}1$ and 2. Two version of the first variant of the initial conditions were assumed. These versions are correspondingly favorable for excitation of the first and the second mode of vibrations. In the process of changing of the modes of vibrations the trajectories of movement, in chosen intervals of time, are very close to the trajectories shown in Figure 3.

4.2.3. *Influence of the torque*

From the linear analysis of a shaft with an applied torque it is possible to show that for a sufficiently high value of the torque, the shaft can lose stability by divergence or by flutter. However, in the case of a shaft which is symmetrically restrained at both ends, e.g., the clamped–clamped case, for the torque values of physical importance one obtains stable solutions which lie inside the stability region. In practice, only by taking into account the internal damping can one show that the self-excited oscillations appear in the system [4].

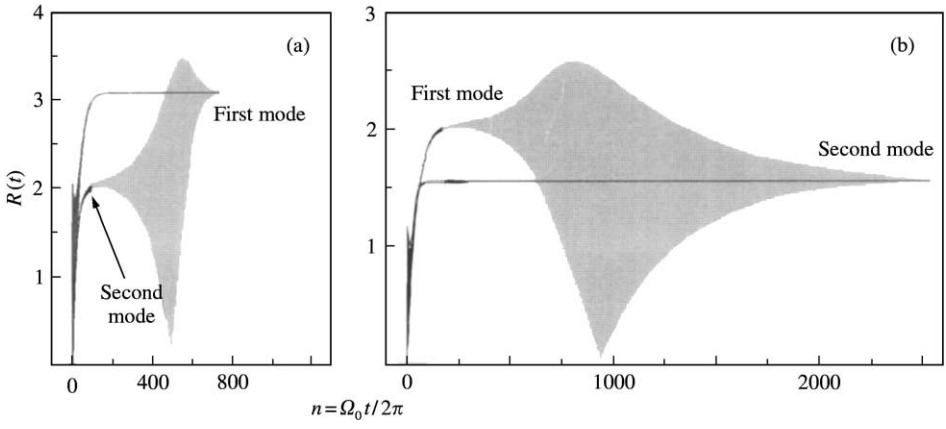

Figure 8. Time histories of R at point $s = l/4$: (a) $\breve{\mu}_i = 0{\cdot}02$, $\breve{\mu}_e = 0{\cdot}002$; (b) $\breve{\mu}_i = 0{\cdot}02$, $\breve{\mu}_e = 0{\cdot}04$.

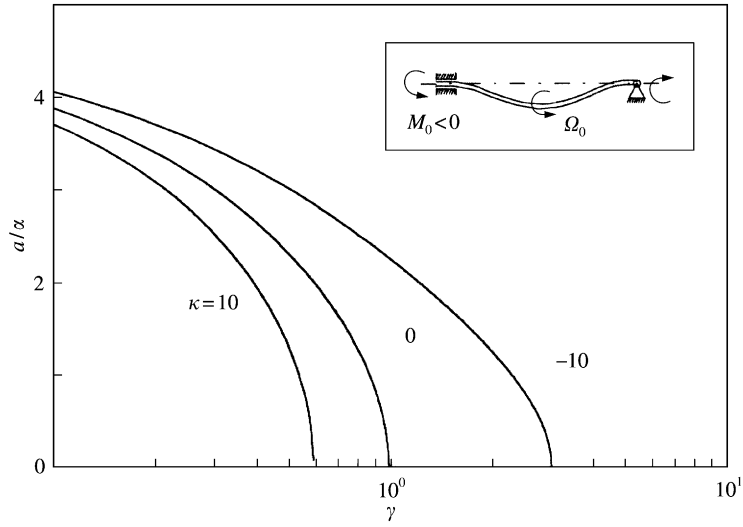

Figure 9. Influence of the torque for clamped–hinged shaft: amplitude versus parameter γ.

For this case, the presence of the torque has only a small effect on the position of the boundaries of the stability region.

A different situation is encountered in the case of a non-symmetrically restrained shaft, e.g., for the case of a shaft clamped at the left end and simply supported at the right end. An important parameter which determines the position of the stability boundaries is the ratio $\kappa = \breve{M}_0/\breve{\mu}_e$ of the non-dimensional torque $\breve{M}_0 = M_0/EI$ to the non-dimensional external damping $\breve{\mu}_e$. The effect of the torque is different depending on its point of application. The result will be different if the torque is applied at the clamped support from the case when it is applied at the simply supported end. The linear analysis of the stability regions indicates that, for small values of external damping, the effect of the torque applied at the clamped end substantially lowers the critical speed.

Figure 9 shows the dependence of the amplitude of vibration on the parameter γ, which characterizes the damping in the system. The results shown have been obtained for the value

of parameter $\beta = 25$ and for the rotation speed $\eta = 2$ which is high enough to ensure that only the first mode can get excited. With increasing the external damping (the parameter γ) the amplitude gets smaller. For positive values of the parameter κ (which corresponds to the case of the torque applied at the simply supported end), for already relatively small values of γ the amplitude of the first mode reaches zero. For negative values of κ, the range of the first mode of self-excited vibration is much broader.

5. CONCLUSIONS

The proposed approach to the modelling of rotating shafts allows for a simple and clear prediction of the matrix equation of motion of the system and proves to be easy to apply in numerical analysis. The application of the Kronecker product to the notation of non-linearities allows one to write the matrix equation of amplitudes which is the base for the prediction of amplitude–frequency dependences for free, forced and self-excited vibrations. The advantages of the way of descriptions and the methods presented in the paper are especially suitable for the coupled flexural, torsional and longitudinal vibrations with the influence of shear and some statical loadings, as well as for slender shafts. By application of these methods it is easy to predict the tangent matrix which can be very helpful in Newton-like methods, and also in detecting bifurcation points and secondary branches of solutions.

The results of the analyses of different dynamic problems for rotating shafts discussed in the paper, confirms the high effectiveness of the method and its applicability especially to some more complex cases difficult to analyze by analytical methods. The results of the calculations have shown some great differences, including qualitative ones, in relation to published papers using Euler-type models.

ACKNOWLEDGMENT

This research was financially supported by Polish Scientific Research Committee PB-0867/T07/2000/19

REFERENCES

1. A. TONDL 1965 *Some Problems of Rotor Dynamics*. London: Chapman & Hall.
2. A. MUSZYŃSKA 1986 *Journal of Sound and Vibration* **110**, 443–462. Whirl and whip-rotor/bearing stability problems.
3. L. W. CHEN and H. C. SHEU 1997 *Journal of Sound and Vibration* **200**, 41–61. The stability behaviour of a non-conservative spinning Timoshenko shaft with an overhung disk.
4. W. KURNIK 1995 *Machine Dynamics Problems* **13**, 7–17. Effect of torque in bifurcation of rotating shaft.
5. J. SHAW and S. W. SHAW 1989 *Journal of Sound and Vibration* **132**, 227–244. Instabilities and bifurcations in a rotating shaft.
6. C. O. CHANG and J. W. CHENG 1993 *Journal of Sound and Vibration* **160**, 433–454. Non-linear dynamics and instability of a rotating shaft–disk system.
7. R. P. HAN and J. W. ZU 1992 *Journal of Sound and Vibration* **156**, 1–16. Modal analysis of rotating shafts: a body-fixed axis formulation approach.
8. H. P. LEE, T. H. TAN and G. S. B. LENG 1997 *Journal of Sound and Vibration* **199**, 401–415. Dynamic stability of spinning Timoshenko shafts with a time-dependent spin rate.
9. E. REISSNER 1981 *Journal of Applied Mathematics and Physics* **32**, 734–744. On finite deformations of space-curved beams.
10. J. C. SIMO and L. VU-QUOC 1986 *Computer Methods in Applied Mechanics and Engineering* **58**, 79–116. A three-dimensional finite strain rod model. Part II: computational aspects.

11. R. LEWANDOWSKI 1997 *International Journal of Solids and Structures* **34**, 1925–1947. Computational formulation for periodic vibration of geometrically nonlinear structures. Part 1: theoretical background.
12. R. LEWANDOWSKI 1997 *International Journal of Solids and Structures* **34**, 1949–1964. Computational formulation for periodic vibration of geometrically nonlinear structures. Part 2: numerical strategy and examples.
13. P. LANCASTER 1969 *Theory of Matrices*. New York and London: Academic Press.
14. R. SEYDEL 1988 *From Equilibrium to Chaos*: *Practical Bifurcation and Stability Analysis* New York: Elsevier.
15. G. SHROFF and H. B. KELLER 1993 *SIAM Journal on Numerical Analysis* **30**, 1099–1120. Stabilization of unstable procedures: the recursive projection method.
16. E. J. DOEDEL, H. B. KELLER and J. P. KERNEVEZ 1991 *International Journal of Bifurcation and Chaos* **1**, 493–520. Numerical analysis and control of bifurcation problems. (I): bifurcation in finite dimensions.
17. E. J. DOEDEL, H. B. KELLER and J. P. KERNEVEZ 1991 *International Journal of Bifurcation and Chaos* **1**(4), 745–772. Numerical analysis and control of bifurcation problems. (II): bifurcation in infinite dimensions.
18. K. MEERBERGEN and D. ROOSE 1996 *IMA Journal of Numerical Analysis* **16**, 297–346. Matrix transformations for computing rightmost eigenvalues of large sparse non-symmetric eigenvalue problems.
19. A. Y. T. LEUNG and T. C. FUNG 1989 *International Journal for Numerical Methods in Engineering* **28**, 1599–1618. Non-linear steady state vibration of frames by finite method.
20. D. ROOSE, K. LUST, A. CHAMPNEYS and A. SPENCE 1995 *Chaos*, *Solitons and Fractals* **5**, 1913–1925. A Newton-Picard shooting method for computing periodic solutions of large-scale dynamical systems.
21. K. ENGELBORGHS, K. LUST and D. ROOSE 1999 *IMA Journal of Numerical Analysis* **19**, 525–547. Direct computation of period doubling bifurcation points of large-scale systems of ODEs using a Newton-Picard method.
22. E. J. DOEDEL 1979 *SIAM Journal on Numerical Analysis* **16**, 173–185. Finite difference collocation methods for nonlinear two point boundary value problems.
23. J. C. SIMO 1985 *Computer Methods in Applied Mechanics and Engineering* **49**, 55–70. A finite strain beam formulation. The three-dimensional dynamic problem. Part I.
24. G. JELENIĆ and M. A. CRISFIELD 1999 *Computer Methods in Applied Mechanics and Engineering* **171**, 141–171. Geometrically exact 3D beam theory: implementation of a strain-invariant finite element for statics and dynamics.
25. L. A. CRIVELLI and C. A. FELIPPA 1993 *International Journal for Numerical Methods in Engineering* **36**, 3647–3673. A three-dimensional non-linear Timoshenko beam based on the core-congruential formulation.
26. A. ARGYRIS 1982 *Computer Methods in Applied Mechanics and Engineering* **32**, 85–155. An excursion into large rotations.
27. J. ŁUCZKO 1998 *Machine Dynamics Problems* **22**, 65–82. A method of analysis of free and forced vibration of continuous systems with quadratic non-linearity.
28. D. J. DAWE and S. WANG 1992 *International Journal for Numerical Methods in Engineering* **33**, 819–844. Vibration of shear-deformable beams using a spline-function approach.
29. M. A. CRISFIELD 1981 *Computers and Structures* **13**, 55–62. A fast incremental-iterative solution procedure that handles snap trough.
30. R. LEWANDOWSKI 1994 *Journal of Sound and Vibration* **177**, 239–249. Solutions with bifurcation points for free vibration of beams: an analytical approach.
31. K. D. MURPHY and C. L. LEE 1998 *Journal of Sound and Vibration* **211**, 179–194. The 1:1 internally resonant response of a cantilever beam attached to a rotating body.
32. P. RIBEIRO and M. PETYT 1999 *Journal of Sound and Vibration* **224**, 591–624. Non-linear vibration of beams with internal resonance by the hierarchical finite-element method.

APPENDIX A

The matrices $\mathbf{A}_i^k$, which describe the linear part of the equations of motion are expressed as

$$\mathbf{A}_2^0 = \mathrm{diag}(\mathbf{B}_1, \mathbf{B}_2, \mathbf{0}, \mathbf{0})$$

$$\mathbf{A}_1^0 = \begin{bmatrix} \mu_e \mathbf{I} & \mathbf{0} & \mathbf{0} & \mathbf{0} \\ \mathbf{0} & \mathbf{B}_g & \mathbf{0} & \mathbf{0} \\ \mathbf{0} & -\mu_i \tilde{\mathbf{e}}_1 & \mathbf{0} & \mathbf{0} \\ \mathbf{0} & \mathbf{0} & \mathbf{0} & \mathbf{0} \end{bmatrix}, \qquad \mathbf{A}_1^1 = \begin{bmatrix} \mathbf{0} & \mathbf{0} & \mathbf{0} & \mathbf{0} \\ \mathbf{0} & \mathbf{0} & \mathbf{0} & \mathbf{0} \\ -\mu_i \mathbf{I} & \mathbf{0} & \mathbf{0} & \mathbf{0} \\ \mathbf{0} & -\mu_i \mathbf{I} & \mathbf{0} & \mathbf{0} \end{bmatrix},$$

$$\mathbf{A}_0^0 = \begin{bmatrix} \mathbf{0} & \mathbf{0} & \mathbf{0} & \mathbf{0} \\ \mathbf{0} & \tilde{\mathbf{N}}_0 \mathbf{e}_1 & -\mathbf{e}_1 & \mathbf{0} \\ \mathbf{0} & -\mathbf{U}\tilde{\mathbf{e}}_1 & \mathbf{J}_1^{-1} & \mathbf{0} \\ \mathbf{0} & \mathbf{0} & \mathbf{0} & \mathbf{J}_2^{-1} \end{bmatrix}, \qquad \mathbf{A}_1^1 = \begin{bmatrix} \mathbf{0} & \tilde{\mathbf{N}}_0 & -\mathbf{I} & \mathbf{0} \\ \tilde{\mathbf{N}}_0 & \tilde{\mathbf{M}}_0 & \mathbf{0} & -\mathbf{I} \\ -\mathbf{U} & \mathbf{0} & \mathbf{0} & \mathbf{0} \\ \mathbf{0} & -\mathbf{U} & \mathbf{0} & \mathbf{0} \end{bmatrix}.$$

It is convenient to write the matrices describing the non-linear terms of the equations of motion in the form

$$\mathbf{F}_{nm}^{ij} = \begin{bmatrix} \mathbf{G}_{nm}^{ij} \\ \mathbf{H}_{nm}^{ij} \end{bmatrix}.$$

Here $\mathbf{G}_{00}^{ij}$, $\mathbf{H}_{00}^{ij}$ describe the non-linearities given by equations (19) and relations (21) respectively. The matrices $\mathbf{G}_{00}^{ij}$ have the form (to simplify notation one omits the argument of the matrix functions $\mathbf{f}_{\alpha\beta}$ when this argument is the unit matrix):

$$\mathbf{G}_{00}^{00} = \begin{bmatrix} \mathbf{0} \\ \mathbf{f}_{32}(\tilde{\mathbf{e}}_1) - \tfrac{1}{2}\tilde{\mathbf{N}}_0 \mathbf{f}_{22}(\tilde{\mathbf{e}}_1) \end{bmatrix}, \qquad \mathbf{G}_{00}^{01} = \begin{bmatrix} \mathbf{f}_{32} - \mathbf{f}_{23} + \mathbf{f}_{22}(\tilde{\mathbf{N}}_0) - \tfrac{1}{2}\tilde{\mathbf{M}}_0 \mathbf{f}_{22} \\ \mathbf{f}_{31} + \mathbf{f}_{42} - \tilde{\mathbf{N}}_0 \mathbf{f}_{21} - \tfrac{1}{2}\tilde{\mathbf{M}}_0 \mathbf{f}_{22} \end{bmatrix},$$

$$\mathbf{G}_{11}^{00} = \begin{bmatrix} \mathbf{0} \\ \mathbf{f}_{22}(\mathbf{B}_2) \end{bmatrix}, \qquad \mathbf{G}_{22}^{00} = \begin{bmatrix} \mathbf{0} \\ \tfrac{1}{2}\mathbf{B}_2 \mathbf{f}_{22} \end{bmatrix}, \qquad \mathbf{G}_{01}^{00} = \begin{bmatrix} \mathbf{0} \\ -\tfrac{1}{2}\mathbf{B}_g \mathbf{f}_{22} \end{bmatrix}.$$

The matrices $\mathbf{G}_{ij}^{kl}$ are given by the following equations:

$$\mathbf{H}_{00}^{00} = \begin{bmatrix} \tfrac{1}{2}\mathbf{f}_{22}(\tilde{\mathbf{e}}_1) + \tfrac{1}{2}\mathbf{g}_{22}(\tilde{\mathbf{e}}_1^2) \\ \mathbf{0} \end{bmatrix}, \qquad \mathbf{H}_{00}^{11} = \begin{bmatrix} -\tfrac{1}{2}\mathbf{g}_{11} - \tfrac{1}{2}\mathbf{g}_{22}(\mathbf{J}_0) \\ -\tilde{\mathbf{e}}_1 \mathbf{U}\mathbf{f}_{21} \end{bmatrix},$$

$$\mathbf{H}_{00}^{01} = \begin{bmatrix} \mathbf{U}\mathbf{f}_{21} + \mathbf{g}_{21}(\tilde{\mathbf{e}}_1) \\ \tfrac{1}{2}\mathbf{U}\mathbf{f}_{22} + \tilde{\mathbf{e}}_1 \mathbf{U}[\tilde{\mathbf{e}}_1 \mathbf{f}_{22} - \mathbf{f}_{22}(\tilde{\mathbf{e}}_1)] \end{bmatrix}.$$

The above expressions can be used, for the assumed Voigt–Kelvin model of damping, to determine the matrices $\mathbf{H}_{10}^{ij}$, $\mathbf{H}_{01}^{ij}$ as

$$\mathbf{H}_{10}^{ij} = \mathbf{H}_{01}^{ij} = \mu_i \mathbf{H}_{00}^{ij}(\mathbf{I})$$

after replacing in all the respective formulae the matrix $\mathbf{U}$ with the unit matrix $\mathbf{I}$.

APPENDIX B: NOMENCLATURE

SCALAR QUANTITIES

E, G, K	Young's and shear moduli, shear factor
ρ	mass density
A, I, l	cross-sectional area, moment of inertia, rod length
α, β	radius of inertia, slenderness co-efficient

μ_i, μ_e	internal and external damping co-efficient
γ	non-dimensional damping parameter
Ω_0, η	rotation speed, non-dimensional rotation speed
N_0, M_0	axial force, torque
ω, ν	frequency, non-dimensional frequency
x_i, $s = x_1$	co-ordinates, natural co-ordinate
t	time

VECTORS (COLUMN MATRICES)

$\mathbf{e}_{j(N)}$, $\mathbf{e}_j = \mathbf{e}_{j(3)}$	unit vector of dimension N
$\mathbf{i}_j$, $\mathbf{g}_j$, $\mathbf{t}_j$	base vectors of a co-ordinate system
$\boldsymbol{\eta}$	displacement vector in the body frame
$\boldsymbol{\omega}$, $\boldsymbol{\Omega}$, $\boldsymbol{\Omega}_0$	angular velocity vectors
$\boldsymbol{\varepsilon}_0$, $\boldsymbol{\varepsilon}_t$, $\boldsymbol{\varepsilon}_r$	strain measure vectors
$\boldsymbol{\varepsilon}$, $\boldsymbol{\sigma}$	vectors made of the components of the strain and stress tensors
$\mathbf{u}$, $\boldsymbol{\phi}$	displacement and rotation vectors
$\mathbf{n}$, $\mathbf{N}$	vectors of internal forces
$\mathbf{m}$, $\mathbf{M}$	vectors of internal moments
$\mathbf{N}_0$, $\mathbf{M}_0$	vectors of constant loads
$\mathbf{x}$, $\mathbf{y}$	state vector
$\mathbf{a}$	amplitude vector
$\mathbf{v}(s)$	vector of shape functions
$\mathbf{w}(t)$	vector of approximating functions

MATRICES

$\tilde{(\cdot)}$	skew-symmetric matrix related to the corresponding vector
$\mathbf{I}_{(N)}$, $\mathbf{I} = \mathbf{I}_{(3)}$	unit matrix of dimension N
$\boldsymbol{\Lambda}$, $\boldsymbol{\Phi}$, $\boldsymbol{\Psi}$	rotation matrices
$\mathbf{A}_k^i$, $\mathbf{A}_k$, $\mathbf{A}$	square matrices describing the linear part of the equation
$\mathbf{F}_{kl}^{ij}$, $\mathbf{F}_{kl}$, $\mathbf{F}$	rectangular matrices describing the non-linear part of the equation
$\mathbf{J}_k$, $\mathbf{B}_k$, $\mathbf{B}_g$	stiffness, inertia and gyroscopic matrices
$\mathbf{E}$	diagonal matrix, depending on Young's and shear moduli